Selective 2′-hydroxyl acylation analyzed by protection from exoribonuclease (RNase-detected SHAPE) for direct analysis of covalent adducts and of nucleotide flexibility in RNA

Kady-Ann Steen, Nathan A Siegfried & Kevin M Weeks

Department of Chemistry, University of North Carolina, Chapel Hill, North Carolina, USA. Correspondence should be addressed to K.M.W. (weeks@unc.edu).

Published online 6 October 2011; doi:10.1038/nprot.2011.373

RNA SHAPE chemistry yields quantitative, single-nucleotide resolution structural information based on the reaction of the 2′-hydroxyl group of conformationally flexible nucleotides with electrophilic SHAPE reagents. However, SHAPE technology has been limited by the requirement that sites of RNA modification be detected by primer extension. Primer extension results in loss of information at both the 5′ and 3′ ends of an RNA and requires multiple experimental steps. Here we describe RNase-detected SHAPE that uses a processive, 3′→5′ exoribonuclease, RNase R, to detect covalent adducts in 5′-end–labeled RNA in a one-tube experiment. RNase R degrades RNA but stops quantitatively three and four nucleotides 3′ of a nucleotide containing a covalent adduct at the ribose 2′-hydroxyl or the pairing face of a nucleobase, respectively. We illustrate this technology by characterizing ligand-induced folding for the aptamer domain of the *Escherichia coli* thiamine pyrophosphate riboswitch RNA. RNase-detected SHAPE is a facile, two-day approach that can be used to analyze diverse covalent adducts in any RNA molecule, including short RNAs not amenable to analysis by primer extension and RNAs with functionally important structures at their 5′ or 3′ ends.

INTRODUCTION

Most RNA molecules form specific secondary and tertiary structures as a prerequisite for carrying out their function[1,2]. Moreover, both large-scale and subtle conformational changes impact the biological roles of many RNAs. Chemical probing technologies have proven to be especially powerful for understanding both global and fine-scale components of RNA structure[3,4]. SHAPE yields quantitative and nucleotide-resolution structural information for RNAs ranging in size from tRNA and small riboswitches[5,6] to entire RNA genomes[7,8]. SHAPE chemistry takes advantage of the discovery that the reactivity of the 2′-hydroxyl position is highly sensitive to the precise conformation of a given nucleotide. Flexible nucleotides adopt many different conformations, a subset of which increases the nucleophilicity of the 2′-hydroxyl group. Electrophilic SHAPE reagents thus react preferentially at dynamic or conformationally flexible nucleotides to form 2′-*O*-adducts. Constrained nucleotides sample fewer conformations and generally show low reactivity with SHAPE reagents (**Fig. 1a**)[5,9].

By using this simple chemical modification reaction, it is possible to obtain a comprehensive view of RNA structure because most RNA nucleotides have a free 2′-hydroxyl, all four nucleotides react similarly with SHAPE reagents[10] and reactivities correlate closely with biophysical measurements of local order in RNA[11]. All SHAPE reagents undergo an auto-inactivating hydrolysis reaction with water (**Fig. 1b**)[9,12]; this self-quenching reaction (with 55 M water) is so dominant that SHAPE chemistry is insensitive to the presence of most common biological buffer components. Thus, SHAPE chemical probing reactions can be performed in the presence of proteins, ligands and other RNAs[6,13–15], as well as in complex biological environments including inside viruses[7,16]. SHAPE reactivity data can be used to inform structure prediction algorithms to generate highly accurate RNA secondary structure models[17].

Primer extension was first used to detect RNA cleavage fragments and covalent adducts resulting from chemical probing experiments over 20 years ago[18,19]. In primer extension, reverse transcriptase enzymes synthesize cDNA from an RNA template. Extension is inhibited when an RNA strand has been cleaved or the RNA base or backbone has been modified such that base-pairing ability is disrupted. Extension is also inhibited if the adduct becomes too large to be accommodated in the polymerase active site. Primer extension coupled with recent innovations, including the use of fluorescently labeled DNA primers, analysis by automated capillary electrophoresis, availability of highly processive polymerases and automated quantification of reactivity patterns, now makes it possible to obtain single-nucleotide resolution structural information for 300–650 nucleotides in a single experiment[4,20,21]. Thus, primer extension is the technology of choice when long read lengths are the primary consideration.

However, detection of RNA adducts by primer extension has important limitations and results in some regions of an RNA being inaccessible to analysis. First, reverse transcriptase–mediated primer extension requires that a DNA oligonucleotide bind at a specific site 3′ to the region of interest. Second, the imperfect processivity of reverse transcriptase during the initial stage of primer extension results in pausing adjacent to the primer binding site. These factors result in a loss of structural data for 40–60 nucleotides at the 3′ end of the RNA. Third, primer extension typically results in a large number of cDNAs that correspond to full-length extension products. These full-length products overlap with and result in a loss of structural data for 5–20 nucleotides at the 5′ end of the RNA. The combined loss of 45–80 nucleotides of data at the 5′ and 3′ ends makes structural analysis of short RNAs in their native forms essentially impossible. The limitations of primer extension–based

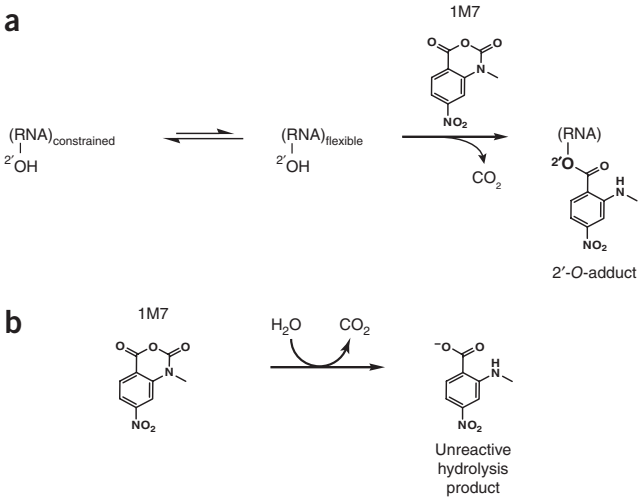

Figure 1 | RNA SHAPE chemistry. (**a**) SHAPE reagents, including 1M7, react preferentially at conformationally flexible nucleotides to form 2′-*O*-adducts. (**b**) Concurrent reagent auto-inactivation by hydrolysis.

structure probing are also evident in longer RNA sequences in which structural data are not obtained at the ends[8,17]. A useful solution to this problem involves appending non-native flanking sequences, a 'structure cassette', on both ends of the RNA to move the region of interest to the readable center of the RNA[22]. Finally, although powerful and highly quantitative, the primer extension process requires multiple biochemical manipulations, RNA-specific primer design, and optimization of annealing and extension conditions.

RNase-detected SHAPE addresses these limitations by using a processive, nonspecific, 3′→5′ exoribonuclease from *Mycoplasma genitalium* (RNase R) to detect covalent adducts in RNA[6]. RNase-detected SHAPE makes possible the direct analysis of RNA fragments that have been chemically modified either by SHAPE reagents that react at the ribose 2′-hydroxyl group or reagents that react at the base-pairing face of nucleobases[6]. The *M. genitalium* RNase R enzyme belongs to the ubiquitous RNR family of exoribonucleases that hydrolytically degrade structured RNAs to release 5′-monophosphates without requiring an exogenous helicase[23–25].

Although a high-resolution structure of the *M. genitalium* RNase R enzyme is not currently available, we can make structural inferences on the basis of homology modeling using the *E. coli* RNase II (ref. 26) and *Saccharomyces cerevisiae* Rrp44 (ref. 27) structures. The RNase R enzyme consists of four major domains: two N-terminal cold-shock domains, CSD1 and CSD2; a central, highly conserved, RNase (RNB) domain; and a C-terminal S1 domain (**Fig. 2**). The RNB domain contains the RNA substrate-binding channel and the active site for hydrolytic degradation of RNA (**Fig. 2**, inset). The RNA strand is threaded to the RNB domain through an opening between the CSD1 and RNB domains (**Fig. 2**, black strand) and makes numerous contacts with protein residues in the RNB domain (**Fig. 2**, inset).

Experimentally, we discovered that RNA fragments containing 2′-*O*-adducts or modifications at the base-pairing face of guanosine are three and four nucleotides longer, respectively, than the actual site of modification[6]. These fragment lengths were determined by comparison with guanosine markers generated by iodine-mediated cleavage of the phosphorothioate-substituted backbone in adduct-free RNAs[6]. The offsets are due to the different contacts made by the 2′-hydroxyl group and the nucleotide base-pairing face of the RNA within the substrate-binding channel of the RNase R enzyme. RNase R glutamic acid residue 463 forms a hydrogen bond with the 2′-hydroxyl group of nucleotide N-3 (**Fig. 2**, red sphere). In contrast, Ser433 makes a hydrogen bond at nucleotide N-4 (**Fig. 2**, blue nucleotide). This 'two-site' model for interactions between the enzyme and the RNA strand is supported by two pieces of data. First, the glutamic acid at position 463 is evolutionarily conserved throughout the RNR enzyme family and interacts with the 2′-hydroxyl of RNA in several family members[26,27]. Mutation of this residue in RNase II from glutamic acid to alanine results in a loss of RNA cleavage specificity[28]. Second, although the residue is not always a serine, a hydrogen-bonding interaction between a residue in the substrate channel and the nucleotide base-pairing face at N-4 is also highly conserved.

RNase-detected SHAPE was previously used to characterize structural transitions induced upon ligand binding to the aptamer domain of the *E. coli* thiamine pyrophosphate (TPP) riboswitch[6]. RNase-detected SHAPE analysis of the TPP riboswitch revealed the secondary structure of the ligand-free state, the nucleotides undergoing the largest conformational changes upon ligand binding and the existence of a single-nucleotide bulge register shift that likely modulates a long-range tertiary interaction. The usefulness of RNase-detected SHAPE is general, and we anticipate that this approach will make possible structural analysis of miRNAs and their precursors, riboswitches and small noncoding RNAs in their native forms. RNase-detected SHAPE will also facilitate the complete analysis of functionally important structures at the 5′ and 3′ ends of large RNAs, including the genomes of RNA viruses.

Experimental design

RNase-detected SHAPE yields quantitative reactivity data for almost every position in an RNA. The technology combines the previously well-characterized SHAPE acylation reaction[9,12,29] with a simple 3′→5′

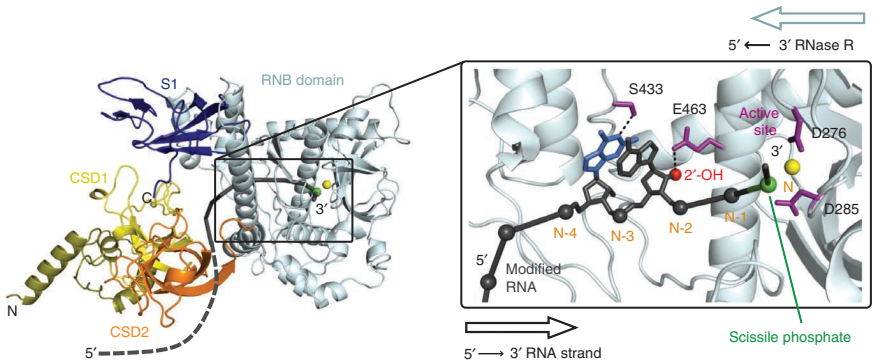

Figure 2 | Model of *M. genitalium* RNase R and the interactions that mediate covalent adduct detection in RNA. The path of the RNA strand (in dark gray) is shown relative to the major enzyme domains. Inset illustrates the substrate-binding channel of the RNase (RNB) domain. Modification of a 2′-hydroxyl group prevents exoribonuclease digestion; the modified residue is shown as a red sphere at N-3. The nucleobase, the base-pairing face of which is recognized by hydrogen bonding with Ser433, is shown in blue at N-4. The site of RNA strand hydrolysis is shown as a green sphere and a catalytic Mg^{2+} ion is yellow. The homology model was generated using I-TASSER[40]. Figure is adapted in part from reference 6.

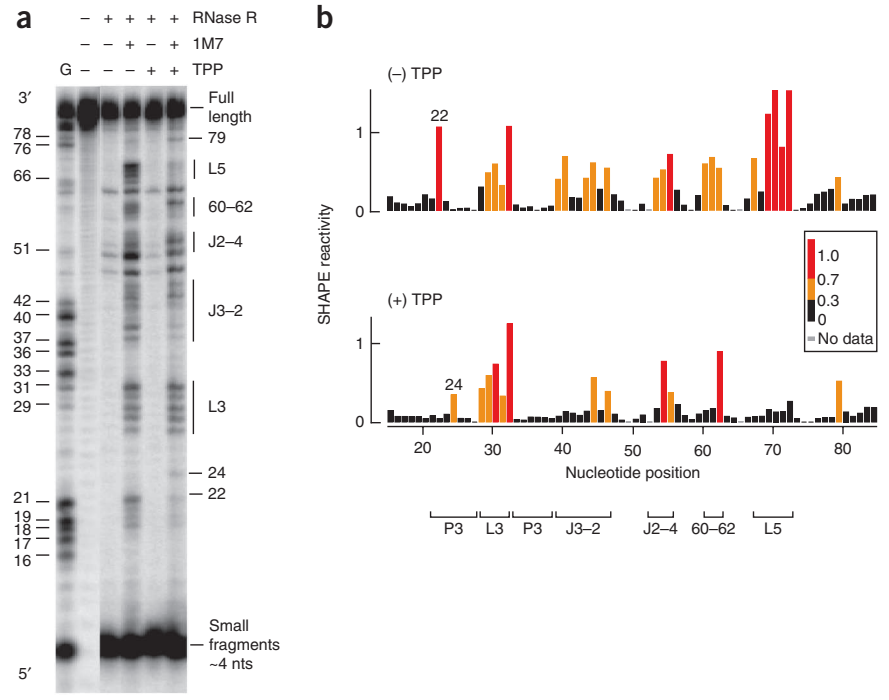

Figure 3 | Representative RNase-detected SHAPE experiment. (**a**) SHAPE reactions, performed using the 1M7 reagent, for the (80-nucleotide) TPP riboswitch domain and kethoxal-mediated sequencing (indicated with a G) resolved by denaturing PAGE. The guanosine sequencing marker is one nucleotide shorter than bands corresponding to the (–) and (+) 1M7 reactions. Guanosine nucleotides are indicated at left; structural landmarks in the RNA are highlighted on the right. (**b**) Absolute SHAPE reactivities in the absence (top) and presence (bottom) of TPP ligand. Columns are colored by individual nucleotide SHAPE reactivities (see scale). SHAPE data are normalized to a scale in which zero indicates no reactivity and 1.0 is defined as the average intensity of highly reactive positions[22] (Step 34).

enzymatic degradation step using a 5′-end–labeled RNA. The current protocol is optimized for highly structured short RNAs (approximately 80–140 nucleotides). However, RNase R digestion temperature and time can be optimized for analysis of longer RNAs. The key experimental variable is that RNase R enzyme activity is strongly sensitive to Mg^{2+} concentration. The optimal range of Mg^{2+} concentration for RNase R activity with structured RNAs is 0.25–0.50 mM. All nucleotide positions, up to and including the 3′ end, can be resolved with sufficiently long electrophoresis times. Information for approximately five nucleotides at the 5′ end of the RNA is obscured because, at the end of digestion, the RNase R enzyme remains bound to the very end of the RNA strand.

RNAs and RNA folding. RNase-detected SHAPE is ideally suited for analysis of short *in vitro* transcripts. This protocol highlights analysis of changes in conformational states that occur upon small molecule binding to a riboswitch RNA and uses an RNA folding approach and buffer conditions that work well for the TPP riboswitch RNA. Other RNAs may require different conditions; essentially, any folding environment appropriate for an RNA of interest can be used. RNase-detected SHAPE can be applied to understanding the changes in RNA folding as a function of temperature, ion concentration and the presence of proteins or ligands. The RNA of interest must be 5′-end labeled[30,31] to facilitate detection of RNase digestion products by electrophoretic separation. In the procedure section we use 5′-[^{32}P]–labeled RNA as an example.

RNA modification. Any SHAPE reagent[9,12,29,32] can be used in RNase-detected SHAPE (for a summary of useful reagents, see ref. 33). For this protocol, we used 1-methyl-7-nitroisatoic anhydride (1M7)[12]. However, any reagent that reacts with an RNA nucleotide and is sufficiently bulky to inhibit movement of the RNA within the RNase R active site (**Fig. 2**) is detectable by this approach. For SHAPE electrophiles, the reagent is added to the folded RNA and allowed to react until inactivation by hydrolysis is complete (**Fig. 1**). SHAPE reagents thus do not require an explicit quench step. For most conventional reagents, a quench step is required; for example, kethoxal is quenched with unbuffered boric acid[18]. In addition, a no-reagent control is performed to account for imperfect digestion by the RNase R enzyme. Once the RNA modification reaction is complete, EDTA is added to chelate free Mg^{2+} and the RNA is recovered by ethanol precipitation to remove buffer components that may inhibit RNase R activity.

RNase R digestion. Sites of 2′-*O*-adduct formation are detected by *M. genitalium* RNase R[23], a 3′→5′ exoribonuclease that (i) is readily heat inactivated[6], (ii) degrades highly structured RNAs and (iii) is inhibited by 2′-*O*-adducts in the substrate RNA. The enzyme is sensitive to Mg^{2+} concentration, so it is critical that Mg^{2+} not be carried over from the chemical modification step. The RNase R enzyme is inactivated by the addition of EDTA and heating at 95 °C for 3 min. A no-reagent, no-enzyme control is performed to identify intrinsic or pre-existing degradation sites in the RNA. The RNA fragments are then recovered by ethanol/isopropanol precipitation, optimized for recovery of small RNA fragments and resolved by denaturing PAGE.

Sequencing. A sequencing lane is used to assign the bands in the (+) and (–) SHAPE reagent lanes. Sequencing lanes are conveniently generated by kethoxal modification of denatured RNA, followed by RNase R degradation of the RNA. Kethoxal covalently modifies single-stranded guanosine residues at the N1 and N2 positions to form a cyclic adduct[18]. SHAPE modification and kethoxal sequencing reactions can be performed concurrently. Kethoxal-mediated sequencing is advantageous because the resulting RNA fragments possess covalent adducts and 3′ ends that are similar to RNase-detected SHAPE fragments. For fragments longer than ~15 nucleotides, RNAs containing SHAPE and kethoxal adducts migrate essentially identically. There are small differences, approximately one-half of a nucleotide, in electrophoretic migration for shorter fragments. In practice, band assignment using kethoxal sequencing ladders is straightforward.

Data analysis and assignment of reactivities. RNase-detected SHAPE yields RNA fragments that terminate three nucleotides 3′ of the site of modification (**Fig. 2**, inset). Kethoxal sequencing, detected by RNase R degradation, yields RNA fragments that terminate four nucleotides 3′ of the kethoxal-modified guanosine nucleotide. Thus, as visualized using 5′-labeled RNA, the kethoxal-mediated guanosine sequencing lanes are exactly one nucleotide shorter than the corresponding 2′-SHAPE adducts (**Fig. 3a**). Band intensities, resolved on sequencing gels, can be conveniently quantified using the Semi-Automated Footprinting Analysis (SAFA) software[34]. SHAPE data are highly reproducible; differences in normalized reactivities between independent replicates are typically less than ±10% and 0.2 absolute SHAPE units.

MATERIALS

REAGENTS

- 5′-[^{32}P]-labeled RNA at a concentration of 0.1 μM or greater in 10 mM HEPES, pH 8.0 ▲ **CRITICAL** RNA preparation must be performed in an RNase-free environment. RNA for modification and RNase R digestion can be stored in aliquots to reduce RNase contamination.
- Glycogen (20 mg ml^{-1}, Roche, cat. no. 901393)
- EDTA (0.5 M, Ambion, cat. no. 9260G)
- Formamide (Acros Organics, cat. no. AC18109)
- DMSO, molecular biology grade (Sigma-Aldrich, cat. no. 115959) ▲ **CRITICAL** DMSO bottle should be stored in a desiccator at room temperature (22 °C).
- 1-Methyl-7-nitroisatoic anhydride (1M7; synthesis is described in refs. 12,35) ▲ **CRITICAL** 1M7 should be stored in a desiccator at 4 °C.
- Kethoxal (USB, cat. no. 17930) ▲ **CRITICAL** Kethoxal should be stored at −20 °C.
- *M. genitalium* RNase R, 4.5 mg ml^{-1}, conveniently obtained by affinity purification using a C-terminal (His)$_6$-tagged expression construct (see **Box 1**, **Supplementary Fig. 1**)
- Thiamine pyrophosphate (TPP; Sigma-Aldrich, cat. no. C8754)
- Boric acid (Sigma-Aldrich, cat. no. B7901)
- SUPERase-In (Ambion, cat. no. AM2694)
- Alkaline phosphatase (Roche, cat. no. 1097075)
- T4 polynucleotide kinase (PNK; New England Biolabs, cat. no. M0201S)
- PNK buffer (10×, New England Biolabs, cat. no. M0201S)
- γ-[^{32}P]-ATP (6 × 106 Ci mol^{-1}, 10 Ci per liter, PerkinElmer, cat. no. BLU502Z)
- Reagents for high-resolution PAGE, including acrylamide/bisacrylamide, 29:1; 7 M urea, 1× TBE
- Phenol/chloroform/isoamyl alcohol (25:24:1) (Acros Organics, cat. no. AC32711-5000)
- Tris (Fisher Bioreagents, cat. no. BP152-5)
- Sodium chloride (NaCl; Fisher Bioreagents, cat. no. BP3581)
- Magnesium chloride ($MgCl_2$; Acros Organics, cat. no. 197530010)
- Potassium chloride (KCl; Fisher Bioreagents, cat. no. BP366-1)
- Ethanol (100%; Fisher Bioreagents, cat. no. BP2818-500)
- Dithiothreitol (DTT; Fisher Bioreagents, cat. no. BP172)
- Sterile water (Ambion, cat. no. AM9930)
- HEPES (Fisher Bioreagents, cat. no. BP2921)

EQUIPMENT

- Amicon Micropure-EZ centrifugal filter devices (Millipore, cat no. 42533)
- −20 °C freezer
- Microcentrifuge for 1.5-ml tubes at 4 °C
- Microcentrifuge tubes
- Reaction tubes (0.65 ml)
- Phosphorimaging instrument and screen
- Gel dryer
- Sequencing apparatus for high-resolution PAGE. We use vertical denaturing gels of dimensions 0.75 mm (length) × 31 cm (width) × 38.5 cm (height) that are prepared using 10–12% (wt/vol) (29:1) acrylamide, 90 mM Tris-borate, 2 mM EDTA and 7 M urea.
- Programmable incubator or heat block

REAGENT SETUP

RNase R stop dye Mix 96% (vol/vol) formamide and 1 mM EDTA, pH 8.0, containing bromophenol blue and xylene cyanol tracking dyes. This solution is stable at 4 °C for at least 3 months.

TE Mix 10 mM Tris and 1 mM EDTA, pH 8.0. This buffer is stable at room temperature for at least 3 months.

RNA folding solution (3.3×) RNA folding solution is prepared by combining 333 mM HEPES, pH 8.0, 333 mM NaCl and 33 mM $MgCl_2$. A wide variety of solution conditions that stabilize the desired structural state of the RNA can be used. Buffer components, ionic strength and ions can all be varied with the proviso that the pH be maintained in the 7.6–8.3 range. In the SHAPE modification reaction, the buffer concentration should be greater than the final reagent concentration. This buffer is stable at room temperature for at least 6 months.

1M7 in DMSO (10×) A good starting 10× 1M7 concentration is 80 mM. The useful range of 10× 1M7 concentration is 15–100 mM. Lower concentrations yield longer read lengths but less intense bands. Freshly prepare this solution before use.

Kethoxal in H_2O (10×) A good starting 10× kethoxal concentration is 20 mM (equal to 1 μl neat kethoxal (7.88 M) in 393 μl H_2O). Freshly prepare this solution before use.

RNase R reaction buffer (10×) RNase R reaction buffer is prepared by combining 200 mM Tris-HCl, pH 8.0, 1 M KCl and 2.5 mM $MgCl_2$. This buffer is stable at room temperature for at least 3 months.

Ligand solution (TPP in $H_2$0), 10× (50 μM)

5′-[32P]-labeled RNA Prepared by carrying out the following steps: (i) Dephosphorylation reaction: Mix 50 mM Tris (pH 8.5), 0.1 mM EDTA, 50 pmol RNA, 300 units SUPERase-In and 200 units alkaline phosphatase in 300 μl total reaction volume. Incubate at 50 °C for 1 h. This solution can be stored at –20 °C for at least 6 months; avoid multiple freeze-thaw cycles. (ii) Phenol/chloroform/isoamyl alcohol extraction, ethanol precipitation and resuspension in TE. (iii) 5′-End labeling: Mix 10 pmol dephosphorylated RNA, 70 mM Tris (pH 7.6), 10 mM $MgCl_2$, 5 mM DTT, 1 μl [γ-^{32}P]-ATP and 2 μl PNK in 20 μl total reaction volume. Incubate at 37 °C for 30 min. (iv) Purify on 8% (wt/vol) denaturing polyacrylamide gel (1× TBE, 7 M urea). Use autoradiography to visualize and excise the band corresponding to the radiolabeled RNA. (v) Passively elute RNA overnight into TE and remove acrylamide pieces using a centrifugal filter device. (vi) Recover radiolabeled RNA by ethanol precipitation (no glycogen should be used if RNA is stored after radiolabeling). Resuspend pellet in 10 mM HEPES, pH 8.0. Resuspended, radiolabeled RNA should be used after preparation to avoid multiple freeze-thaw cycles. Radiolabeled RNA can be stored in single-use aliquots at −20 °C for 2–3 weeks. Fluorescently labeled RNA should be stored in a similar manner. Alternatively, 5′-fluorescently labeled RNAs can be used; for labeling protocols, see refs. 30,31.

BOX 1 | PURIFICATION OF THE *M. GENITALIUM* RNASE R ENZYME

The *rnr* gene of *M. genitalium* G37 codes for RNase R; this coding region was previously adapted for expression in *E. coli* by Lalonde *et al.*[23]. Using this construct (a generous gift of the laboratory of Zhongwei Li), we placed the coding region in a pET-21d (EMD Biosciences) vector to add a C-terminal $(His)_6$ tag for affinity purification. This supporting protocol presents a streamlined purification for this affinity-tagged RNase R protein construct.

RNase R can be handled safely in an RNA lab if care is taken to prevent cross-contamination with other experiments. RNase R purification should be carried out in an isolated lab area. Glassware and other items should be sequestered for 'RNase use only.' Bench paper should be used and disposed of immediately after use (as should all RNase-related waste). Reactions containing RNase R are readily inactivated by heating to 95 °C for 3 min in the presence of EDTA[6].

REAGENTS

- pET-21d(+) plasmid vector containing the *M. genitalium* RNase R coding sequence
- One Shot BL21(DE3) chemically competent *E. coli* (Invitrogen, cat. no. C6000-03)
- LB Broth, Miller (LB; Fisher, cat. no. BP1426-500)
- LB Agar, Miller (Fisher, cat. no. BP1425-500)
- SOC Medium (Invitrogen, 15544-034)
- Isopropyl-β-D-galactopyranoside, 1 M (IPTG; Fisher, cat. no. BP-1620)
- Ampicillin, sodium salt, 100 mg ml^{-1} (Amp; Fisher, cat. no. BP1760)
- Glycerol (Fisher, cat. no. BP229-1)
- β-Mercaptoethanol (β-ME; EMD, cat. no. 444203)
- Imidazole (Acros Organics, cat. no. 122025000)
- DTT, 1 M (Fisher, cat. no. BP172-25)
- NaCl (Fisher, cat. no. BP 3581)
- Ni^{2+}-NTA Resin (5Prime, cat. no. 24000)
- SDS-PAGE reagents (Invitrogen, Novex)

REAGENT SETUP

- **LB**, autoclaved (a total of 3 liters is required; 2 liters in 4-liter baffled flasks, 1 liter in a glass bottle)
- **LB-amp plates**, containing 100 μg ml^{-1} ampicillin
- **Lysis buffer, low salt** (50 mM Tris, pH 7.8, 300 mM NaCl, 5% (vol/vol) glycerol), prepare 500 ml
- **Lysis buffer, high salt** (50 mM Tris, pH 7.8, 700 mM NaCl, 5% (vol/vol) glycerol), prepare 1 liter
- **TE** (10 mM Tris, 1 mM EDTA, pH 8.0)
- **Dialysis buffer** (40 mM Tris, pH 7.5, 250 mM NaCl, 2 mM DTT, 50% (vol/vol) glycerol), DTT should be added immediately before use; prepare 4 liters
- **Imidazole buffer** (3.4 g imidazole, pH to 8 with HCl, 2.5 ml of 1 M Tris (pH 7.8), 0.875 g NaCl, 3.13 ml 80% (vol/vol) glycerol), prepare 50 ml and filter-sterilize

EQUIPMENT

- Sonicator
- SDS-Page apparatus (XCell SureLock MiniCell CE; Invitrogen)
- Stir plate
- Floor centrifuge (Sorvall, SS34 and GS3 rotors)
- Shaker
- Labquake tube rotator at 4 °C
- Tabletop centrifuge with 50-ml conical tube adaptors at 4 °C
- Sterile Petri dishes
- Autoclave
- Two 4-liter autoclaved baffled flasks
- Autoclaved centrifuge bottles and tubes, 500 and 50 ml for SS34 and GS3 rotors
- Beakers, 100 and 200 ml
- Round-bottom tubes, 14 ml (Thermo Scientific, cat. no. 150268)
- Float-A-Lyzer G2 dialysis tubes, 50,000-Da molecular weight cutoff (Spectrum, G235058)
- Heat block

PROCEDURE

RNase R Expression ● TIMING 2–3 d

1| Transform pET-21d plasmid vector into competent *E. coli* BL21(DE3) cells. If using One Shot BL21 cells, add 1 μl of plasmid to one tube of cells, mix gently, chill cells on ice for 5 min, heat shock at 42 °C for exactly 30 s without mixing and then place cells on ice for 5 min. Add 250 μl of room temperature SOC and shake at 37 °C for 1 h to allow expression of antibiotic resistance gene.

2| Plate several dilutions of transformed cells on pre-warmed LB-amp plates and incubate at 37 °C overnight.

3| The following morning, remove the plates from the incubator and store at 4 °C until evening to prevent overgrowth.

4| Inoculate two culture tubes containing 5 ml of LB with one colony each, add 5 μl of 100 mg ml^{-1} ampicillin. Incubate in a shaker overnight at 250 r.p.m. and 37 °C.

5| The following morning, warm two 4-liter baffled flasks containing 1 liter of LB each to 37 °C. Inoculate each flask with a 5-ml overnight culture, add 1 ml of 100 mg ml^{-1} ampicillin and immediately take an optical density reading at 600 nm (OD_{600}).

(continued)

BOX 1 | CONTINUED

6| Incubate flasks by shaking at 250 r.p.m. at 37 °C. Monitor until OD_{600} is ~0.5. Remove a 500-µl sample, mark 'uninduced' and freeze. Add 1 ml of 1 M IPTG to each 1 liter of culture in order to induce expression of RNase R. Reduce the temperature to 25 °C.
▲ **CRITICAL STEP** RNase R expression is substantially enhanced if overexpression is carried out at 25 °C rather than at 37 °C.
7| Continue incubation for 5 h. Remove a 500-µl aliquot, label 'induced' and store at −20 °C.
8| Pellet cells by spinning at 3,400*g* for 15 min in two 500-ml centrifuge bottles. Multiple spins will be required to pellet 2 liters of cell culture in these two bottles. After the first spin, discard the supernatant and refill the centrifuge bottle with cell culture and spin again. At the end of this process, each bottle will contain a pellet corresponding to 1 liter of the LB culture.
■ **PAUSE POINT** Cell pellets can be stored at −80 °C overnight.

Purification of RNase R ● TIMING 2 d

1| Thaw frozen pellets on ice for 15 min.
2| Add 175 µl and 350 µl of fresh β-ME to the low- and high-salt lysis buffers, respectively.
3| Resuspend each pellet in 6.25 ml of low-salt lysis buffer.
4| Combine suspended pellets into one 50-ml glass beaker, place the beaker into a larger beaker containing an ice and water bath and sonicate. Be careful not to heat the *E. coli* sample while sonicating. Cycle 15 s sonication and 30 s rest until sample viscosity and color are reduced.
5| Remove a 500-µl aliquot, label 'cell lysate' and store at −20 °C.
6| Centrifuge for 30 min at 39,000*g* in a SS34 rotor (Thermo Scientific) to clear the lysate and then pour the supernatant into a clean centrifuge bottle and repeat.
7| During centrifugation, prepare the Ni^{2+}-NTA resin. Stir the resin into slurry immediately before pipetting, as it will quickly settle. Add 20 ml of slurry to a 50-ml Falcon tube; spin at 350*g* for 1 min in a tabletop clinical centrifuge (at 4 °C). Remove and discard the supernatant.
8| To exchange resin buffer, add 5 ml of low-salt lysis buffer to the Ni^{2+}-NTA resin, then place the tube in a tube rocker (also at 4 °C) and allow the resin to mix for 5 min. Centrifuge the tube at 350*g*; remove and discard the supernatant. Repeat two more times.
9| Retrieve cleared lysate from the centrifuge, remove a 500-µl aliquot, label as 'supernatant' and store at −20 °C. Apply the remaining supernatant to the prepared nickel resin and rock the tube for 90 min.
10| Centrifuge the tube at 350*g* for 1 min, remove and save the supernatant, label as 'flowthrough' and place on ice.
11| In a 300-ml beaker, combine 200 ml of high-salt lysis buffer and 4 ml of imidazole buffer. This combined solution (wash buffer, containing ~20 mM imidazole) will be used to wash the resin three times. Add 30 ml of wash buffer to the resin and rock the tube for 10 min. Centrifuge at 350*g* for 1 min, remove and save the supernatant, label as 'Wash 1' and place on ice.
12| As in Step 11, add 30 ml of wash buffer to the resin, rock the tube for 10 min, centrifuge at 350*g* for 1 min, and remove and save the supernatant as 'Wash 2.' Repeat for Wash 3.
13| In a 100-ml beaker combine 50 ml of high-salt lysis buffer and 20 ml of imidazole buffer to prepare the elution buffer (containing 286 mM imidazole). Add 10 ml of this solution to the resin and rock the tube for 30 min. Spin as above. Remove and save the supernatant as 'Elution 1.'
14| Add another 10 ml of elution buffer to the resin as in Step 13. Repeat Step 13; save supernatant as 'elution 2.'
15| Pipet enzyme samples into Float-A-Lyzer G2 dialysis tubes and dialyze against 400 ml of low-salt lysis buffer for 2 h.
16| Prepare 4 liters of dialysis buffer by adding DTT to a final concentration of 2 mM, then add 2 liters of this buffer to a large beaker on a magnetic stir plate at 4 °C. Save a 1-ml aliquot of dialysis buffer to serve as a blank for quantifying enzyme concentration.
17| Transfer dialysis tubes to the beaker, dialyze for 8 h, replace dialysis buffer and dialyze overnight.
18| Quantify protein concentration using a sample of the final dialysis buffer as a blank when obtaining the protein absorbance. The extinction coefficient (at 280 nm) for the RNase R enzyme is 62,000 M^{-1} cm^{-1} (ref. 23). This procedure typically yields an enzyme solution of 5–12 µg $µl^{-1}$; however, it is important to ensure that the enzyme stock concentration is at or above the experimentally useful concentration of 4.5 µg $µl^{-1}$ (ref. 6).

SDS-PAGE Analysis ● TIMING 90 min, overnight

1| Results of the RNase R purification procedure should be evaluated by analysis of the aliquots collected throughout this protocol by SDS-PAGE. Any appropriate gel electrophoresis system can be used. We typically use the Novex System (Invitrogen). Gel analysis should be carried out according to standard denaturing protein gel protocols (for example, see ref. 41). Samples to be analyzed include uninduced cells, induced cells (from the addition of IPTG), lysate, supernatant, washes 1, 2 and 3, and elutions 1 and 2.
2| To lyse uninduced and induced samples prior to analysis, first centrifuge at 10,000*g* for 5 min, decant and discard supernatant.
3| Resuspend pellets in 75 µl of a gel loading buffer containing SDS, add 75 µl of TE and then add 1.5 µl of β-ME (1% (vol/vol) final).
4| Heat the two samples at 90 °C for 5 min, vortex briefly and then centrifuge the resuspended cells at 14,000*g* for 10 min.
5| Prepare each of the other samples by combining 75 µl of sample with 75 µl of SDS gel loading buffer. Heat at 90 °C for 5 min, vortex and spin briefly.
6| Load samples (~13 µl each) and a standard protein size ladder onto the gel and then run at 150 V for ~1 h.
7| The protein content of each sample can be visualized by Coomassie or silver staining[3].
8| Dry the gel to maintain a permanent record. A representative gel showing purification of the *M. genitalium* RNase R (75,000 kDa) is shown in **Supplementary Figure 1**. The enzyme is typically ≥95% homogenous as judged by size, and it contains no detectable non-RNase R activity.

PROCEDURE

RNA folding ● TIMING 40 min

1| Add 1 pmol (~10,000 cpm) of 5′-[^{32}P]–labeled RNA in 24 µl of sterile H_2O to a 0.65-ml reaction tube.

2| Heat the RNA to 95 °C for 2 min, then immediately place on ice for 2 min.

3| Add 12 µl of 3.3× folding solution and mix.

4| Incubate the tube at the desired reaction temperature (25 or 37 °C) for 10 min.

5| Preincubate a 0.65-ml reaction tube containing 2 µl of 10× ligand solution (TPP) or H_2O.

6| Add 18 µl of prefolded RNA to 2 µl of 10× ligand solution (TPP) or H_2O (in this example, the TPP riboswitch is probed in the ligand-free and ligand-bound states).

? TROUBLESHOOTING

7| Incubate the tube at the desired reaction temperature (25 or 37 °C) for 20 min.

RNA structure modification ● TIMING 1.5 h

8| Aliquot 1 µl of 10× 1M7 in DMSO (for the (+) 1M7 reaction) and 1 µl of neat DMSO (for the (−) 1M7 reaction (control)) into 0.65-ml reaction tubes.

9| Remove 9 µl of folded RNA and add to (+) and (−) 1M7 reactions. Mix thoroughly and incubate the reaction at 25 °C for 1.33 min or at 37 °C for 1.25 min. This is equivalent to five 1M7 hydrolysis half-lives[12].

? TROUBLESHOOTING

10| After the reaction has proceeded to completion, recover the RNA by ethanol precipitation. To each tube (a total of four), add 2.5 µl of 100 mM EDTA (to chelate Mg^{2+}), 90 µl of sterile H_2O, 5 µl of 4 M NaCl, 1 µl of 20 mg ml^{-1} glycogen and 380 µl of 100% ethanol; mix, then incubate at −20 °C for 30 min. Precipitate the RNA by spinning at maximum speed in a microcentrifuge at 4 °C for 30 min.

▲ **CRITICAL STEP** The activity of *M. genitalium* RNase R is very sensitive to Mg^{2+} concentration. It is essential to remove all Mg^{2+} from the RNA modification (structure probing) step prior to the RNase R detection step.

? TROUBLESHOOTING

11| Remove ethanol supernatant and resuspend each RNA sample in 8 µl of sterile H_2O.

■ **PAUSE POINT** The modified RNA can be stored at −20 °C overnight.

Kethoxal modification (performed concurrently with 1M7 modification)

12| Add 0.1 pmol of 5′-[^{32}P]-labeled RNA in 16 µl of sterile H_2O to a 0.65-ml reaction tube.

13| Heat the RNA to 95 °C for 2 min, and then immediately place on ice for 2 min.

14| Add 2 µl of 1 M HEPES (pH 8.0) and mix thoroughly.

15| Incubate the tube at 70 °C for 3 min.

16| Preincubate a 0.65-ml reaction tube containing 2 µl of 20 mM kethoxal in sterile H_2O at 70 °C for 1 min.

17| Add the RNA to the kethoxal solution and mix well.

18| Incubate at 70 °C for 5 min.

? TROUBLESHOOTING

19| Quench reaction with 20 µl of 10 mM unbuffered boric acid.

20| Recover the RNA by ethanol precipitation. Add 60 µl of sterile H_2O, 10 µl of 4 M NaCl, 1 µl of 20 mg ml^{-1} glycogen and 380 µl of 100% ethanol; mix, then incubate at −20 °C for 30 min. Precipitate the RNA by spinning at maximum speed in a microcentrifuge at 4 °C for 30 min.

21| Remove ethanol supernatant and add 400 µl 70% (vol/vol) ethanol. Invert the tube to dislodge and wash pellet. Recover RNA by spinning at maximum speed in a microcentrifuge at 4 °C for 2 min.

22| Repeat Step 21.

23| Resuspend RNA in 8 µl of sterile H_2O.
■ **PAUSE POINT** The modified RNA can be stored at −20 °C overnight.

RNase R digestion ● TIMING 2 h
24| Add 1 µl of 10× RNase R reaction buffer to RNAs from Steps 11 and 23.

25| Add 1 µl of *M. genitalium* RNase R (4.5 mg ml^{-1}) to each tube and mix well.
▲ **CRITICAL STEP** Use aerosol-resistant tips for all steps involving pipetting active RNase R and solutions containing this enzyme prior to the heat-inactivation step.

26| Incubate tubes at 50 °C for 30 min.
▲ **CRITICAL STEP** RNA secondary structure is destabilized at elevated temperatures, which facilitates RNase R degradation of structured RNAs[6,36].
? TROUBLESHOOTING

27| Add 1 µl of 100 mM EDTA and incubate at 95 °C for 3 min to inactivate RNase R.
▲ **CRITICAL STEP** RNase R is irreversibly inactivated by heat[6]. This inactivation step is especially important to prevent RNase contamination when working in an RNA lab.

28| Recover RNA fragments by ethanol/isopropanol precipitation. To each tube, add 90 µl of sterile H_2O, 10 µl of 4 M NaCl, 100 µl of 100% isopropanol, 250 µl of 100% ethanol and mix; incubate at −20 °C for 30 min. Precipitate the RNA by spinning at maximum speed in a microcentrifuge at 4 °C for 45 min. Alternatively, samples can be loaded directly onto the gel without ethanol/isopropanol precipitation. However, precipitation reduces the total volume, concentrates the intensity of the 5′ label and removes salt and buffer components to yield improved gel resolution.
▲ **CRITICAL STEP** Isopropanol is required to efficiently precipitate smaller RNA fragments. Omitting this step leads to loss of RNA fragments shorter than ~15 nucleotides.
? TROUBLESHOOTING

29| Remove the supernatant and resuspend the pellet in 7–9 µl of RNase R stop dye.

30| Heat at 95 °C for 3 min.
■ **PAUSE POINT** Samples can be stored at −20 °C overnight.

RNA fragment analysis by gel electrophoresis ● TIMING ~7 h
31| Load ~2 µl of each reaction (~5,000 cpm) into individual lanes of a 10% (wt/vol) polyacrylamide sequencing gel (29:1 acrylamide/bisacrylamide, 1× TBE, 7 M urea). To resolve both the 5′ and 3′ ends of the RNA, perform electrophoresis for 90 min at 70 W, and then reload the same samples in unoccupied lanes on the gel and continue electrophoresis for 150 min at 70 W. The samples loaded first will have been subjected to electrophoresis for ~240 min, which will resolve nucleotides close to the 3′ end of the RNA, whereas samples loaded later will provide data on the 5′ region.
? TROUBLESHOOTING

32| Dry the gel using a heated vacuum gel dryer for ~1 h.
? TROUBLESHOOTING

33| Expose the gel overnight to a phosphor screen and quantify scanned bands using a phosphorimaging instrument. Quantify the intensity of every well-defined band in the gel for the (+) and (−) 1M7 lanes by 2D densitometry using SAFA[34].

34| Calculate the absolute SHAPE reactivity at each position in the RNA by subtracting the (−) 1M7 intensities from the (+) 1M7 intensities. In general, the data are normalized by excluding the top 2% of the reactive nucleotides, averaging the next 10% of reactive nucleotides and then dividing all intensities by this averaged value[22] (**Supplementary Data 1**). For longer RNAs, it may be necessary to correct for signal decay, as described[7,13].
The guanosine sequencing lanes generated by RNase R-detected kethoxal modification are exactly one nucleotide shorter than the corresponding sites of 1M7 modification.

? TROUBLESHOOTING

Troubleshooting advice can be found in **Table 1**.

TABLE 1 | Troubleshooting table.

Step	Problem	Possible reason	Solution
6	Nucleotide transitions associated with ligand binding are not observed, (+) and (−) ligand states are identical	Ligand binding is not occurring	Increase ligand concentration
9	Low or no signal in (+) 1M7 lane	Insufficient modification of RNA	Perform modification using a twofold higher concentration of 1M7 Ensure that 1M7 stock is kept dry—trace amounts of water will react with reagent. Make sure DMSO stock solution is also kept dry. Make fresh 1M7 solution for each experiment
	Bands observed close to the 3′ end of the RNA (top of gel), but no small RNA fragments observed	Excessive modification of RNA	Perform structure modification step using a twofold lower concentration of reagent
10, 26	Very low signal in the (+) 1M7 lane and an intense full-length RNA band is observed	Poor or inefficient RNase R digestion	RNase R is very sensitive to Mg^{2+} concentration—ensure that final divalent ion concentration is 0.25 mM. Use desalting columns after modification. Use fresh stock of RNase R if enzyme activity is low. Increase enzyme concentration or digestion time
18	Some guanosine residues are not detected in the kethoxal sequencing lane	Complete kethoxal modification prevented by RNA folding	Repeat kethoxal modification step at 90 °C to ensure that RNA is denatured
	No sequencing bands in kethoxal lane	Insufficient kethoxal modification of RNA	Increase kethoxal concentration and/or reaction time. Make fresh kethoxal solution for each experiment
26	Bright bands observed in (−) and (+) 1M7 lanes that do not correspond to modification stops or RNase contamination	Structure-induced pausing by RNase R enzyme	Heat RNA in sterile H_2O to 95 °C for 3 min, and place tube on ice. Add enzyme and incubate tube immediately at 50 °C. Increase digestion time
28	No small oligonucleotide fragments in any lane	Loss of small fragments during ethanol precipitation	Add glycogen to ethanol/isopropanol precipitation step. Increase incubation time at −20 °C. Increase spin time in microcentrifuge
31	Bright bands present in the (−) 1M7 lane	RNase contamination, most commonly caused by endonucleases. This problem can occur at any step in the protocol.	Identify contaminated solution using an RNase detection kit or by evaluating each step of the protocol by resolving a labeled test RNA on a denaturing gel
	Low band intensities in all lanes	5′-[^{32}P]–labeled RNA does not have sufficient specific activity	Repeat with freshly prepared [^{32}P]-labeled RNA
		Not enough 5′-[^{32}P]–labeled RNA used for each experiment	Repeat with a higher concentration of RNA

(continued)

TABLE 1 | Troubleshooting table (continued).

Step	Problem	Possible reason	Solution
	The faintest bands in the (+) 1M7 lane have significantly different intensities as compared with the corresponding bands in the (−) 1M7 lanes	Random error involved with volume measurement; gel loaded unevenly	Small differences in background intensity can be accounted for by statistical normalization (Step 34). If intensities are significantly different, the gel should be rerun by loading samples with similar amounts of RNA in each lane
	Low resolution of bands in all lanes (smearing)	Overloading of gel lane	Reduce the volume or concentration of RNA loaded onto gel
		Uneven heating of gel during electrophoresis	Ensure that electrophoresis equipment works well
		Excess salt present in samples before loading on gel	Perform additional 70% (vol/vol) ethanol wash. Use desalting columns after RNase R digestion
32		Gel drying is not effective	Ensure that the gel dryer seals properly

● **TIMING**

Steps 1–7: 40 min
Steps 8–11 and 12–23: 1.5 h (done concurrently)
Steps 24–30: 2 h
Step 31: ~4 h
Steps 32–34: 3 h plus time necessary to expose screen

ANTICIPATED RESULTS

RNase-detected SHAPE makes possible single-nucleotide analysis of local nucleotide flexibility for most nucleotides in an RNA, including those at the 5′ and 3′ ends. The experiment is conducted in a single reaction tube and yields direct and experimentally straightforward detection of RNA covalent adducts.

The representative experiment described here was conducted using an 80-nucleotide *in vitro* transcript corresponding to the aptamer domain of the TPP-sensing riboswitch from the *E. coli thiM* mRNA[37]; no flanking sequences were added. The TPP RNA structure was probed in both the ligand-free and ligand-bound states. Kethoxal-mediated sequencing at guanosine nucleotides was used to assign bands observed in the (+) and (−) SHAPE reagent lanes (**Fig. 3a**). Bands at the top of the gel correspond to undigested full-length RNA and larger RNA fragments that are not fully resolved in this particular electrophoresis run (**Fig. 3a**). Bright bands at the bottom of the gel are short oligonucleotide fragments that reflect the short RNA 'handle' by which RNase R binds RNA, and correspond to the end products of 3′→5′ exoribonuclease digestion. Using RNase R-detected SHAPE, we resolved and quantified SHAPE reactivities for both the ligand-free and the ligand-bound riboswitch RNA states (**Fig. 3b**).

RNase-detected SHAPE accurately recapitulates the previously characterized base-pairing pattern and tertiary structure interactions of the TPP-bound state[37]. Regions that are directly involved in TPP binding (J3-2 and nts 60–61, **Figs. 3b** and **4b,c**) are constrained and unreactive in the ligand-bound state. The prominent long-range tertiary interaction involving the L5 loop binding to the P3 helix results in low SHAPE reactivities for the loop nucleotides (**Fig. 3b**).

RNase-detected SHAPE also revealed that the riboswitch aptamer domain undergoes significant conformational changes upon TPP binding as previously reported[6] (compare (−) and (+) TPP reactions, **Fig. 3**). The SHAPE data support a specific, nucleotide resolution, secondary structure model for the ligand-free state[6]. The ligand-free state forms an open Y-conformation in which unreactive helices (P2–P5) are linked together by relatively reactive and thus conformationally flexible joining regions (J2–4, J3–2 and nucleotides 60–62; **Fig. 4a**).

Comparing the SHAPE-supported ligand-free and ligand-bound states reveals changes that are consistent with previously described large-scale structural changes associated with ligand binding[37–39] (see J3–2 and nts 60–61, **Fig. 4**). In addition to these changes, RNase-detected SHAPE uniquely reveals important fine-scale changes. For example, SHAPE detects formation of the A53–A84 noncanonical base pair in the ligand-bound state (**Fig. 4**). In addition, RNase-detected SHAPE reveals a single-nucleotide register shift in the P3 helix upon ligand binding. In the ligand-free state, C22 is reactive and is likely to be a single-stranded bulge; however, in the ligand-bound state C24 is reactive, whereas C22 is unreactive. Thus, C24 forms a bulged structure in the TPP-bound state (**Fig. 4**). This register shift likely has an important structural role because C24 mediates a stacking interaction with A69 (refs. 37,39), a nucleotide that contributes to docking of the loop nucleotides in L5 with the P3 helix.

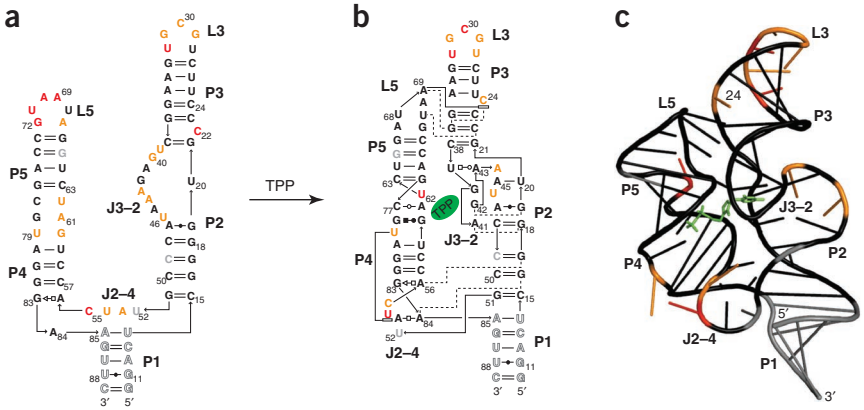

Figure 4 | Structural transitions in the TPP riboswitch aptamer domain visualized by RNase-detected SHAPE. (**a**,**b**) Absolute SHAPE reactivities are superimposed on secondary structure models for the riboswitch RNA in the absence (**a**) and presence (**b**) of TPP ligand. (**c**) Tertiary structure[37] of the TPP-bound state. Nucleotides are colored by SHAPE reactivity using the scale shown in **Figure 3**. Nucleotides that are not probed in this experiment are shown in gray. Portions of this figure were reproduced with permission from ref. 6.

Superposition of SHAPE reactivities on the 3D structure for the TPP-bound RNA riboswitch domain emphasizes the tight packing of this RNA. Although this RNA contains numerous regions that are depicted as single stranded in a secondary structure diagram, many of these elements are constrained by noncanonical local interactions or interactions with the TPP ligand and are unreactive (**Fig. 4c**, nucleotides in black). The core of the TPP riboswitch aptamer domain is tightly packed and highly constrained. Locally flexible nucleotides, as measured by SHAPE, lie almost exclusively at the exterior of the structure (**Fig. 4c**, emphasized in orange and red).

RNase-detected SHAPE allows quantitative, single-nucleotide detection of covalent adducts at the 2′-OH position and at base-pairing faces of the nucleobases using an adduct-inhibited 3′→5′ exoribonuclease, RNase R. RNase R–mediated detection is simple to implement and should be broadly applicable for detection of diverse classes of covalent adducts in RNA. RNase-detected SHAPE will allow for direct single-nucleotide structural analysis of previously inaccessible RNAs, especially short noncoding RNAs and RNAs with functionally important structures at their 5′ and 3′ ends.

Note: Supplementary information is available via the HTML version of this article.

ACKNOWLEDGMENTS We are indebted to A. Malhotra for many productive discussions regarding the mechanism of RNase R enzymes and to Z. Li for the gift of a plasmid encoding *M. genitalium* RNase R optimized for expression in *E. coli*. We thank P. Homan for helpful discussions regarding synthesis of 1M7. This work was supported by a grant from the National Science Foundation (MCB-0919666 to K.M.W.); N.A.S. is a Fellow of the UNC Lineberger Comprehensive Cancer Center.

AUTHOR CONTRIBUTIONS K.-A.S. and K.M.W. collaborated on all aspects of the conception and writing of this paper. N.A.S. and K.M.W. wrote the Supporting Protocol on RNase R purification.

COMPETING FINANCIAL INTERESTS The authors declare no competing financial interests.

Published online at http://www.natureprotocols.com/.
Reprints and permissions information is available online at http://www.nature.com/reprints/index.html.

1. Gesteland, R.F., Cech, T.R. & Atkins, J.F. *The RNA World* (Cold Spring Harbor Laboratory Press, 2004).
2. Li, P.T., Vieregg, J. & Tinoco, I. Jr. How RNA unfolds and refolds. *Annu. Rev. Biochem.* **77**, 77–100 (2008).
3. Brunel, C. & Romby, P. Probing RNA structure and RNA-ligand complexes with chemical probes. *Methods Enzymol.* **318**, 3–21 (2000).
4. Weeks, K.M. Advances in RNA structure analysis by chemical probing. *Curr. Opin. Struct. Biol.* **20**, 295–304 (2010).
5. Wilkinson, K.A., Merino, E.J. & Weeks, K.M. RNA SHAPE chemistry reveals nonhierarchical interactions dominate equilibrium structural transitions in tRNA(Asp) transcripts. *J. Am. Chem. Soc.* **127**, 4659–4667 (2005).
6. Steen, K.A., Malhotra, A. & Weeks, K.M. Selective 2′-hydroxyl acylation analyzed by protection from exoribonuclease. *J. Am. Chem. Soc.* **132**, 9940–9943 (2010).
7. Wilkinson, K.A. *et al.* High-throughput SHAPE analysis reveals structures in HIV-1 genomic RNA strongly conserved across distinct biological states. *PLoS Biol.* **6**, e96 (2008).
8. Watts, J.M. *et al.* Architecture and secondary structure of an entire HIV-1 RNA genome. *Nature* **460**, 711–716 (2009).
9. Merino, E.J., Wilkinson, K.A., Coughlan, J.L. & Weeks, K.M. RNA structure analysis at single nucleotide resolution by selective 2′-hydroxyl acylation and primer extension (SHAPE). *J. Am. Chem. Soc.* **127**, 4223–4231 (2005).
10. Wilkinson, K.A. *et al.* Influence of nucleotide identity on ribose 2′-hydroxyl reactivity in RNA. *RNA* **15**, 1314–1321 (2009).
11. Gherghe, C.M., Shajani, Z., Wilkinson, K.A., Varani, G. & Weeks, K.M. Strong correlation between SHAPE chemistry and the generalized NMR order parameter (S^2) in RNA. *J. Am. Chem. Soc.* **130**, 12244–12245 (2008).
12. Mortimer, S.A. & Weeks, K.M. A fast-acting reagent for accurate analysis of RNA secondary and tertiary structure by SHAPE chemistry. *J. Am. Chem. Soc.* **129**, 4144–4145 (2007).
13. Badorrek, C.S. & Weeks, K.M. Architecture of a gamma retroviral genomic RNA dimer. *Biochemistry* **45**, 12664–12672 (2006).
14. Duncan, C.D. & Weeks, K.M. Nonhierarchical ribonucleoprotein assembly suggests a strain-propagation model for protein-facilitated RNA folding. *Biochemistry* **49**, 5418–5425 (2010).
15. Wang, B., Wilkinson, K.A. & Weeks, K.M. Complex ligand-induced conformational changes in tRNA(Asp) revealed by single-nucleotide resolution SHAPE chemistry. *Biochemistry* **47**, 3454–3461 (2008).
16. Gherghe, C. *et al.* Definition of a high-affinity Gag recognition structure mediating packaging of a retroviral RNA genome. *Proc. Natl. Acad. Sci. USA* **107**, 19248–19253 (2010).
17. Deigan, K.E., Li, T.W., Mathews, D.H. & Weeks, K.M. Accurate SHAPE-directed RNA structure determination. *Proc. Natl. Acad. Sci. USA* **106**, 97–102 (2009).
18. Ehresmann, C. *et al.* Probing the structure of RNAs in solution. *Nucleic Acids Res.* **15**, 9109–9128 (1987).
19. Stern, S., Moazed, D. & Noller, H.F. Structural analysis of RNA using chemical and enzymatic probing monitored by primer extension. *Methods Enzymol.* **164**, 481–489 (1988).
20. Mitra, S., Shcherbakova, I.V., Altman, R.B., Brenowitz, M. & Laederach, A. High-throughput single-nucleotide structural mapping by capillary automated footprinting analysis. *Nucleic Acids Res.* **36**, e63 (2008).
21. McGinnis, J.L., Duncan, C.D. & Weeks, K.M. High-throughput SHAPE and hydroxyl radical analysis of RNA structure and ribonucleoprotein assembly. *Methods Enzymol.* **468**, 67–89 (2009).

22. Wilkinson, K.A., Merino, E.J. & Weeks, K.M. Selective 2′-hydroxyl acylation analyzed by primer extension (SHAPE): quantitative RNA structure analysis at single nucleotide resolution. *Nat. Protoc.* **1**, 1610–1616 (2006).
23. Lalonde, M.S. *et al.* Exoribonuclease R in Mycoplasma genitalium can carry out both RNA processing and degradative functions and is sensitive to RNA ribose methylation. *RNA* **13**, 1957–1968 (2007).
24. Vincent, H.A. & Deutscher, M.P. The roles of individual domains of RNase R in substrate binding and exoribonuclease activity. The nuclease domain is sufficient for digestion of structured RNA. *J. Biol. Chem.* **284**, 486–494 (2009).
25. Matos, R.G., Barbas, A. & Arraiano, C.M. RNase R mutants elucidate the catalysis of structured RNA: RNA-binding domains select the RNAs targeted for degradation. *Biochem. J.* **423**, 291–301 (2009).
26. Frazao, C. *et al.* Unravelling the dynamics of RNA degradation by ribonuclease II and its RNA-bound complex. *Nature* **443**, 110–114 (2006).
27. Lorentzen, E., Basquin, J., Tomecki, R., Dziembowski, A. & Conti, E. Structure of the active subunit of the yeast exosome core, Rrp44: diverse modes of substrate recruitment in the RNase II nuclease family. *Mol. Cell* **29**, 717–728 (2008).
28. Barbas, A. *et al.* Determination of key residues for catalysis and RNA cleavage specificity: one mutation turns RNase II into a 'SUPER-ENZYME'. *J. Biol. Chem.* **284**, 20486–20498 (2009).
29. Mortimer, S.A. & Weeks, K.M. Time-resolved RNA SHAPE chemistry. *J. Am. Chem. Soc.* **130**, 16178–16180 (2008).
30. Qin, P.Z. & Pyle, A.M. Site-specific labeling of RNA with fluorophores and other structural probes. *Methods* **18**, 60–70 (1999).
31. Bakin, A.V., Borisova, O.F., Shatsky, I.N. & Bogdanov, A.A. Spatial organization of template polynucleotides on the ribosome determined by fluorescence methods. *J. Mol. Biol.* **221**, 441–453 (1991).
32. Gherghe, C.M., Mortimer, S.A., Krahn, J.M., Thompson, N.L. & Weeks, K.M. Slow conformational dynamics at C2′-endo nucleotides in RNA. *J. Am. Chem. Soc.* **130**, 8884–8885 (2008).
33. Weeks, K.M. & Mauger, D.M. Exploring RNA structural codes with SHAPE chemistry. *Acc. Chem. Res.* **44** (26 May 2011).
34. Das, R., Laederach, A., Pearlman, S.M., Herschlag, D. & Altman, R.B. SAFA: semi-automated footprinting analysis software for high-throughput quantification of nucleic acid footprinting experiments. *RNA* **11**, 344–354 (2005).
35. Steen, K.A., Siegfried, N.A., & Weeks, K.M. Synthesis of 1-methyl-7-nitroisatoic anhydride (1M7). *Protoc. Exch.* Published online, doi:10.1038/protex.2011.255.
36. Vincent, H.A. & Deutscher, M.P. Insights into how RNase R degrades structured RNA: analysis of the nuclease domain. *J. Mol. Biol.* **387**, 570–583 (2009).
37. Serganov, A., Polonskaia, A., Phan, A.T., Breaker, R.R. & Patel, D.J. Structural basis for gene regulation by a thiamine pyrophosphate-sensing riboswitch. *Nature* **441**, 1167–1171 (2006).
38. Lang, K., Rieder, R. & Micura, R. Ligand-induced folding of the thiM TPP riboswitch investigated by a structure-based fluorescence spectroscopic approach. *Nucleic Acids Res.* **35**, 5370–5378 (2007).
39. Kulshina, N., Edwards, T.E. & Ferre-D'Amare, A.R. Thermodynamic analysis of ligand binding and ligand binding-induced tertiary structure formation by the thiamine pyrophosphate riboswitch. *RNA* **16**, 186–196 (2010).
40. Zhang, Y. I-TASSER server for protein 3D structure prediction. *BMC Bioinformatics* **9**, 40 (2008).
41. Schagger, H. Tricine-SDS-PAGE. *Nat. Protoc.* **1**, 16–22 (2006).